

Varicella-Zoster Virus Infection Triggers Formation of an Interleukin-1 β (IL-1 β)-processing Inflammasome Complex*

Received for publication, December 8, 2010, and in revised form, March 7, 2011. Published, JBC Papers in Press, March 8, 2011, DOI 10.1074/jbc.M110.210575

Adel M. Nour^{†1}, Mike Reichelt[‡], Chia-Chi Ku[§], Min-Yin Ho[§], Thomas C. Heineman[¶], and Ann M. Arvin[‡]

From the [‡]Departments of Pediatrics and Microbiology and Immunology, Stanford University School of Medicine, Stanford, California 94305, [§]The Graduate Institute of Immunology, College of Medicine, National Taiwan University, Taipei, Taiwan, and [¶]GlaxoSmithKline Biologicals, King of Prussia, Pennsylvania 19101

Innate cellular immunity is the immediate host response against pathogens, and activation of innate immunity also modulates the induction of adaptive immunity. The nucleotide-binding oligomerization domain (NOD)-like receptors (NLRs) are a family of intracellular receptors that recognize conserved patterns associated with intracellular pathogens, but information about their role in the host defense against DNA viruses is limited. Here we report that varicella-zoster virus (VZV), an alphaherpesvirus that is the causative agent of varicella and herpes zoster, induces formation of the NLRP3 inflammasome and the associated processing of the proinflammatory cytokine IL-1 β by activated caspase-1 in infected cells. NLRP3 inflammasome formation was induced in VZV-infected human THP-1 cells, which are a transformed monocyte cell line, primary lung fibroblasts, and melanoma cells. Absent in melanoma gene-2 (AIM2) is an interferon-inducible protein that can form an alternative inflammasome complex with caspase-1 in virus-infected cells. Experiments in VZV-infected melanoma cells showed that NLRP3 protein recruits the adaptor protein ASC and caspase-1 to form an NLRP3 inflammasome complex independent of AIM2 protein and in the absence of free radical reactive oxygen species release. NLRP3 was also expressed extensively in infected skin xenografts in the severe combined immunodeficiency mouse model of VZV pathogenesis *in vivo*. We conclude that NLRP3 inflammasome formation is an innate cellular response to infection with this common pathogenic human herpesvirus.

Varicella-zoster virus (VZV),² also known as human herpesvirus 3, is a highly contagious ubiquitous human herpesvirus

that causes varicella (chickenpox) upon primary infection and zoster (shingles) upon reactivation of latent virus from sensory ganglia (1, 2). Herpesviruses have double-stranded DNA genomes; the VZV genome is the smallest (~125,000 bp) among the human herpesviruses, encoding about 70 open reading frames (ORFs), and is closely related to herpes simplex viruses (HSVs) 1 and 2.

VZV infection is known to elicit the production of cytokines associated with innate cellular responses (3, 4). Mammalian cells have pattern recognition receptors that recognize either conserved pathogen-associated molecular patterns or danger-associated molecular patterns and trigger these intrinsic cellular responses. Many DNA viruses have been reported to be recognized by intracellular and extracellular pattern recognition receptors (5–8). The two major groups of pattern recognition receptors are the toll-like receptors, which survey the extracellular space, and the nucleotide-binding oligomerization domain (NOD)-like receptors (NLRs), which sense pathogen-associated molecular patterns and danger-associated molecular patterns in the intracellular space (9, 10). The NLRs are a large family of cytosolic pattern recognition receptors; 23 NLRs have been identified in the human genome, and the mouse genome has 34 NLRs (11, 12).

Caspase-1 activation is evidence of NLR signaling that has resulted in formation of a functional inflammasome complex within the cell. The inflammasome typically consists of the NLR, procaspase-1, and adaptor molecules (10). In addition to the signal provided by the pathogen, this multiprotein complex, which is necessary to drive the activation of caspase-1, requires intracellular potassium ion pumping; when potassium efflux is prevented, inflammasome activation is abolished in response to most known signals (12–15).

Only three NLR family members are known to form inflammasomes in human cells; these are NLRP1 (NALP1), NLRP3 (NALP3), and NLRC4 (ICE (interleukin-1 converting enzyme) protease-activating factor). Once activated, inflammasomes function in the innate response against microbes by catalyzing the processing of the inflammatory cytokines interleukin (IL)-1 β , IL-18, and probably IL-33 and target a broad range of cellular proteins (16–18). Depending on the cell type and the strength of the activation signal, active caspase-1 has functions that vary from promoting the survival pathway (17) to inducing cell death (19). IL-1 β induction is an important initial host defense mechanism when cells encounter viral and bacterial pathogens. In the context of the innate cellular response to microbes, the proteolytic effect of active caspase-1 on IL-1 β

* This work was supported, in whole or in part, by National Institutes of Health Grants AI20459 and AI053846 and Grant CA49605 from the NCI.

⌘ Author's Choice—Final version full access.

¹ To whom correspondence should be addressed: Depts. of Pediatrics and Microbiology and Immunology, S-366, Stanford University School of Medicine, 300 Pasteur Dr., Stanford, CA 94305-5208. Tel.: 650-725-6555; Fax: 650-725-9828; E-mail: adelmn@stanford.edu.

² The abbreviations used are: VZV, varicella-zoster virus; NLR, nucleotide-binding oligomerization domain (NOD)-like receptor; SCID, severe combined immunodeficiency; HSV, herpes simplex virus; ASC, apoptosis-associated specklike containing a caspase-activating and recruitment domain; AIM2, absent in melanoma gene-2; ROS, reactive oxygen species; HELF, human lung embryonic fibroblast; Boc-D-CMK, *t*-butoxycarbonyl-aspartic acid benzyl ester-chloromethyl ketone; PMA, phorbol 12-myristate 13-acetate; MxA, myxovirus resistance protein-1; CM-H₂DCFDA, 5-(and-6)-chloromethyl-2',7'-dichlorodihydrofluorescein diacetate, acetyl ester; dsDNA, double-stranded DNA.

VZV Triggers Inflammasome Formation

and its secretion are evidence of the enzymatic activity of the inflammasome in the infected cell.

The NLRP3 inflammasome, which is formed by multimerization of NLRP3, apoptosis-associated specklike containing a caspase-activating and recruitment domain (ASC) protein, NAIP, CIITA, HET-E and TP1 containing domain, and procaspase-1, is the best characterized human inflammasome complex. NLRP3 contains a C-terminal leucine-rich repeat domain homologous to that of the toll-like receptors, a central nucleotide-binding and oligomerization domain (NAIP, CIITA, HET-E and TP1 containing domain), and an N-terminal pyrin domain, which recruits ASC protein to the inflammasome. The adaptor protein ASC contains a pyrin domain and a caspase recruitment domain that recruit caspase-1 to the NLRP3 complex (10, 20).

In addition to the pathway involving NLR-containing inflammasomes, caspase-1 activation can occur by a mechanism in which the absent in melanoma gene-2 (AIM2) protein functions as a sensor for cytosolic DNA in a complex with ASC (21). AIM2 is a type 1 interferon (IFN)-induced protein. The AIM2/ASC mechanism is independent of NLR proteins but also results in caspase-1-mediated processing of pro-IL-1 β to its mature form. AIM2/ASC inflammasome formation with caspase-1 activation has been described recently in cells infected with vaccinia virus, a large double-stranded DNA virus that replicates exclusively in the cytoplasm (8).

In this study, we report that VZV infection induced formation of the NLRP3 inflammasome and that this response was elicited in three different cell types that are permissive for VZV replication, including primary human lung fibroblasts, melanoma cells, and the THP-1 monocyte cell line. Caspase-1 activation occurred via a mechanism that was independent of reactive oxygen species (ROS) release and type 1 interferon-mediated AIM2 expression. NLRP3 was induced during VZV infection of human skin xenografts in our severe combined immunodeficiency (SCID) mouse model of VZV pathogenesis, indicating that this innate response is triggered when human epidermal and dermal cells are infected with a human herpesvirus *in vivo*.

EXPERIMENTAL PROCEDURES

Cells and Viruses—Human lung embryonic fibroblasts (HELFs) and human melanoma (MeWo) cells (ATTC) were grown in Dulbecco's modified Eagle's medium supplemented with 10% fetal bovine serum (FBS), 100 μ M nonessential amino acids, and antibiotics (100 units/ml penicillin and 100 μ g/ml streptomycin). The THP-1 cell line (ATTC) was grown in RPMI 1640 medium supplemented with 50 μ M β -mercaptoethanol, 10% fetal bovine serum, 100 μ M nonessential amino acids, and antibiotics (100 units/ml penicillin and 100 μ g/ml streptomycin). VZV (recombinant parent Oka) (22) and rOka-ORF10-GFP were propagated in HELF, melanoma, and THP-1 cells. VZV-infected cells were used to inoculate uninfected cells at a ratio of 1:2, 1:5, or 1:10. HSV-1 infection was done with cell-free virus at a multiplicity of infection of 10.

The recombinant VZV, rOka-ORF10-GFP, expressing ORF10 as an ORF10-GFP fusion protein was constructed from VZV cosmids (23). The 9145-bp SpeI fragment from the pvFsp4 cosmid was cloned into Bluescript to make pBS-9190. A BglII site

was introduced into ORF10 in the pBS-9190 plasmid (CGCG (bp 13385–13388) to GATC) by site-directed mutagenesis. To make the recombinant virus with green fluorescence protein (GFP) at the C terminus of ORF10, enhanced GFP with BglII linkers (generated by PCR) was inserted into the novel BglII site such that enhanced GFP is expressed after amino acid 408 of ORF10. Transfection of the mutated cosmid with the three intact cosmids yielded rOka-ORF10-GFP; the recombinant virus had the same growth kinetics and plaque morphology as the parent. The expected ORF10-GFP insertion was confirmed by sequencing, and the virus expressed GFP in melanoma cells.

For the inflammasome inhibition assay, HELFs were mock-infected or infected with VZV for 24 h, and 1 μ g/ml lipopolysaccharide (LPS) (Sigma-Aldrich) was added for 2 h before measuring IL-1 β . Mock- or VZV-infected cells treated with LPS were incubated with the caspase-1 inhibitor Boc-D-CMK (EMD Chemicals) at 50 μ M (final concentration) for 1 h, with 130 mM KCl (final concentration) for 2 h, or with 10 μ M MG132 (EMD Chemicals) for 2 h before measuring IL-1 β .

For transfection with poly(dA:dT), THP-1 and MeWo cells were grown in 6-well plates in RPMI 1640 medium and DMEM, respectively. THP-1 cells were induced to differentiate with 50 ng/ml PMA (Sigma-Aldrich) for about 6 h. Cells were washed with phosphate-buffered saline (PBS) and transfected with 1 μ g/ml poly(dA:dT) (Sigma-Aldrich) in Opti-MEM (Invitrogen) using Lipofectamine 2000 (Invitrogen). For treatment with ATP/LPS, THP-1 cells were grown in 6-well plates in RPMI 1640 medium and induced with 50 ng/ml PMA (Sigma) for about 6 h before adding 10 μ g/ml LPS (Sigma-Aldrich) overnight, and 5 mM ATP (Sigma-Aldrich) was added for 1 h. For IFN- α treatment, MeWo cells were grown in DMEM and treated with 1000 units/ml IFN- α (Sigma-Aldrich) for 12 h.

IL-1 β Assays—Secreted IL-1 β in supernatants from cells infected with VZV or HSV-1 was measured by enzyme-linked immunosorbent assay (ELISA) according to the manufacturer's recommendation (eBioscience). Samples were tested in triplicate, and data were analyzed using Prism 5 software.

Antibodies—Antibodies used for immunoblots were rabbit polyclonal anti-caspase-1 (p20) (Cell Signaling Technology), anti-caspase-1 (p10) (Santa Cruz Biotechnology), anti-ASC (Enzo Life Sciences), anti-AIM2 (Abcam), anti-myxovirus resistance protein-1 (MxA) (24), mouse anti-NLRP3 (Abcam), rabbit anti-IL-1 β (Cell Signaling Technology), and mouse anti- β -actin (Santa Cruz Biotechnology). Antibodies used for confocal microscopy and immunohistochemistry were rabbit anti-NLRP1 (Abcam), mouse monoclonal anti-VZV-IE62 (Millipore), rabbit polyclonal anti-VZV-ORF23, rabbit anti-VZV-IE63 (a gift from William Ruyechan, University of Buffalo), and rabbit polyclonal anti-VZV-ORF29 (a gift from Saul Silverstein, Columbia University). Antibodies for secondary detection were Alexa Fluor 488-, 594-, or 647-conjugated donkey anti-mouse or donkey anti-rabbit antibody (Invitrogen).

Immunoaffinity Purification—Immunopurification of the caspase-1 complex was done as described previously (25). Briefly, 1 mg of the caspase-1 (p10) antibody was incubated with 1 ml of protein A-Sepharose beads (Invitrogen) with continuous mixing at 4 $^{\circ}$ C for 2 h. The beads were then centrifuged and washed five times with PBS and once with 200 mM sodium

borate, pH 9. Equal volumes of 40 mM dimethyl suberimidate (Sigma) in 200 mM sodium borate were mixed with the beads, and the suspension was incubated for 30 min with continuous mixing. The reaction was terminated by adding an equal volume of 400 mM ethanolamine, and the sample was incubated for an additional 30 min. The beads were packed into a 1-cm-diameter column (Bio-Rad) and washed three times with 2 bed volumes of PBS and once with 4 bed volumes of 100 mM glycine-HCl at pH 2.4 to remove non-cross-linked antibodies. Finally, the cross-linked antibody beads were washed with PBS until the pH reached 7 and stored at 4 °C in PBS containing 0.02% sodium azide. To reduce nonspecific protein-protein interactions, test samples were precleared with protein A beads cross-linked to total IgG from preimmune rabbit serum (Sigma-Aldrich) and purified rabbit IgG without exposure to human caspase-1 antigen. Infected and control uninfected cells were trypsinized and lysed with 1% Nonidet P-40, 150 mM NaCl, 50 mM Tris, pH 8.4 in the presence of protease inhibitors (Roche Applied Science). Eluates from the affinity column were concentrated using a 10-kDa-cutoff Amicon Ultra-4 concentrator (Millipore).

SDS-Polyacrylamide Gel Electrophoresis and Western Blot Analysis—Caspase-1 activation and other immunoblot assays were performed using HELF, melanoma, and THP-1 cells infected with VZV (recombinant pOka) as follows. Cells were washed with PBS and lysed in radioimmunoprecipitation assay buffer (50 mM Tris-HCl, pH 7.4, 0.1% sodium dodecyl sulfate (SDS), 0.5% sodium deoxycholate, 1% Nonidet P-40, 150 mM NaCl, 1 mM EDTA) containing a protease inhibitor mixture (Roche Applied Science). Cell lysates were then centrifuged at 10,000 rpm for 15 min, and about 15 μ g of protein was run on 4–20% SDS-polyacrylamide gradient gels (Bio-Rad). Immunoblotting was performed with antibody dilutions recommended by the manufacturers.

Flow Cytometry—Melanoma cells were infected with VZV ORF10-GFP virus (one infected cell to five uninfected cells) for 24 h, and CellTracker Red CMPTX was added (Invitrogen). THP-1 cells were added to the monolayer of infected melanoma cells and incubated for 24 h, collected, and stained for cell viability (live/dead staining dye; Invitrogen). As a control, uninfected THP-1 cells were stained with CellTracker Red CMPTX. CellTracker Green BODIPY was used to stain THP-1 cells as a positive control for the GFP signal. Using these markers, VZV-infected THP-1 cells were sorted, grown overnight in RPMI 1640 medium, and checked for viability. The transmission of VZV from infected THP-1 cells was assessed by adding infected THP-1 to uninfected HELF (1:10 ratio) cells. Cells were incubated for about 4 days, and HELF infection was monitored by fluorescence microscopy.

Fluorescence Microscopy—The immunostaining procedures were performed as described previously (25). Briefly, about 4×10^5 HELF cells/ml were grown overnight on coverslip Lab-Tek II chambers (Nalgene). Infected THP-1 cells were induced with 50 ng/ml PMA for about 6 h. Mock- and VZV-infected melanoma and HELF cells were incubated with the biotinylated YVAD inhibitor (AnaSpec) at a final concentration of 10 μ M for 1 h at 37 °C. Cells were stained with Hoechst 33342 (10 μ g/ml) for 15 min, washed twice with PBS, fixed with 4% paraformaldehyde for 10 min, and permeabilized with 1% Triton X-100 in PBS. Fixed cells were incubated for about 30 min at room tem-

perature in the presence of 2 μ g/ml streptavidin-conjugated Texas Red (Jackson ImmunoResearch Laboratories), washed five times with PBS at room temperature, and examined using a Leica TCS^{SP2} confocal laser scanning microscope (Heidelberg, Germany). For antibody immunostaining, fixed cells were blocked with 10% fetal bovine serum in PBS and then incubated with the desired primary antibody for 1 h at room temperature. Cells were then washed 10 times with PBS, incubated with secondary antibodies (30 min), washed, and mounted using Paramount (Invitrogen). Controls included nonmatching secondary antibodies and secondary antibodies alone. Cells were imaged with the Leica TCS^{SP2} confocal microscope.

Electron Microscopy (EM)—EM was done as described previously (26). Briefly, THP-1 cells were grown and infected with sorted VZV-infected THP-1 cells in a 6-well plate for 24 h, and cells were recovered, centrifuged, washed with PBS three times, gently pelleted, and fixed in 4% paraformaldehyde and 2% glutaraldehyde in phosphate buffer (0.1 M, pH 7.2). Cells were postfixated with 1% osmium tetroxide (2 h) and incubated in 1% aqueous uranyl acetate overnight. The samples were dehydrated in a series of increasing ethanol concentrations followed by a final propylene oxide step. The samples were embedded in Embed812 (Electron Microscopy Sciences). Ultrathin sections (60 nm) were prepared with a diamond knife (Diatome) and an ultramicrotome (Ultracut, Leica). Sections were stained with 3.5% aqueous uranyl acetate for 10 min and with 0.2% lead citrate for 3 min. The sections were analyzed using a JEOL 1230 transmission electron microscope at 80 kV, and digital photographs were taken with a Gatan Multiscan 701 digital camera.

ROS Release Assay—Melanoma cells were infected with VZV for 24 h, trypsinized, washed with PBS, stained with the ROS release sensor CM-H₂DCFDA (Invitrogen), and evaluated for ROS release by FACSCaliber (BD Biosciences). As a positive control, uninfected melanoma cells were treated with 100 μ M H₂O₂ (final concentration) for an hour.

Analysis of VZV Skin Lesions—VZV infection of human skin xenografts in SCID mice and the analysis of tissue sections were done as described previously (27). Briefly, skin xenografts were made in homozygous CB-17^{SCID/SCID} mice using human fetal tissue obtained according to federal and state regulations; animal use was approved by the Stanford University Administrative Panel on Laboratory Animal Care. For immunohistochemistry analysis of NLRP3 expression, formalin-fixed, paraffin-embedded skin sections (5 μ m) were deparaffinized, rehydrated, treated with antigen retrieval reagent (Vector Laboratories), and treated with 3% hydrogen peroxidase. Sections were incubated with NLRP3 antibody, biotinylated anti-rabbit secondary antibody, and HRP-conjugated streptavidin (Lab Vision). Signals were developed with Vector VIP chromogen (purple) and counterstained with methyl green (Vector Laboratories). VZV was detected with a high titer human polyclonal anti-VZV serum. For confocal microscopy to assess NLRP3 expression, 5- μ m sections of infected human skin were deparaffinized, rehydrated, and subjected to antigen retrieval using the pressure cooker method in the presence of 10 mM sodium citrate, pH 6. Sections were blocked with 0.5% fish gelatin and stained with anti-NLRP3 (Abcam); secondary antibody alone was used as a control. The lesion area was

VZV Triggers Inflammasome Formation

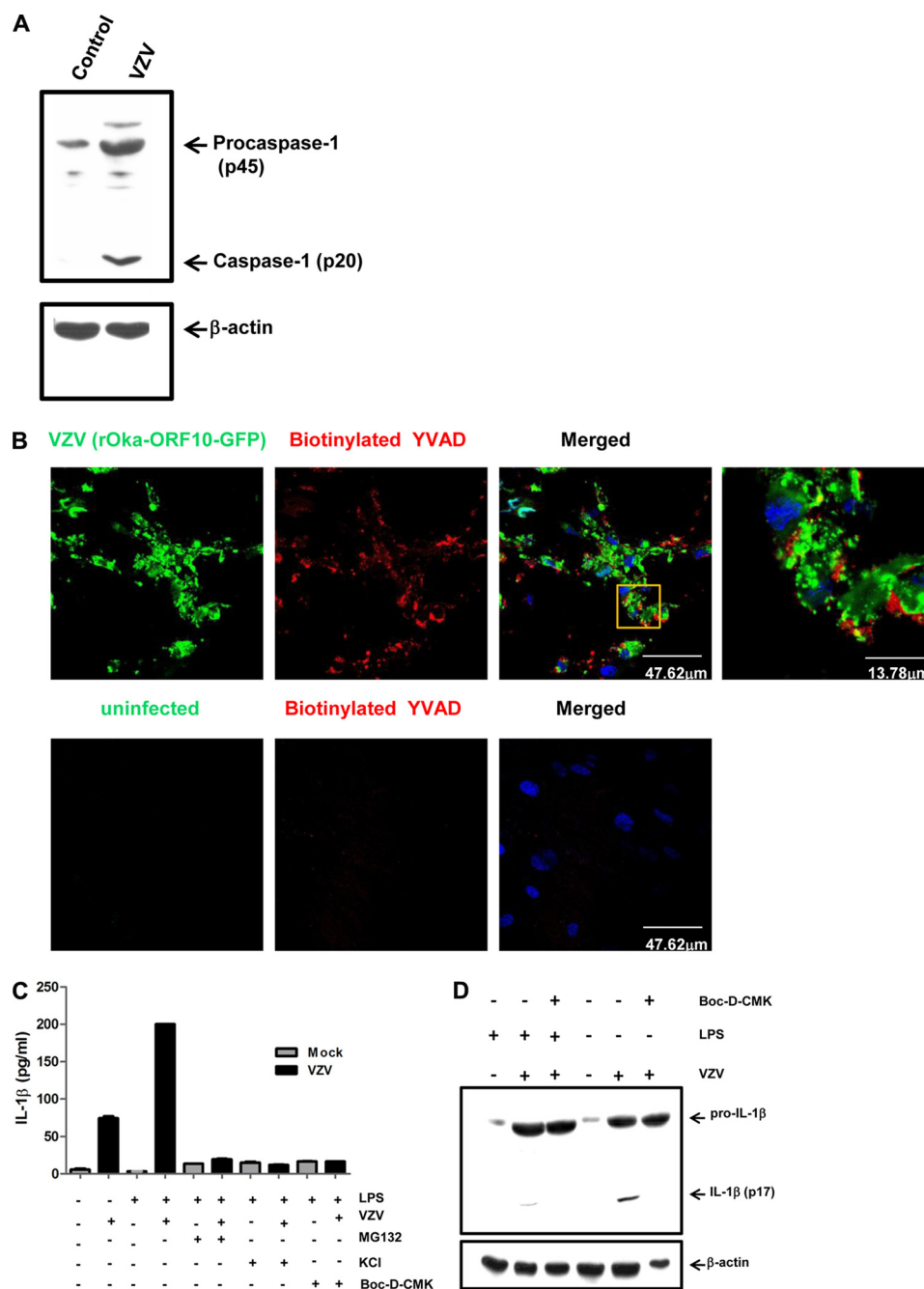


FIGURE 1. Activation of caspase-1 in VZV-infected HELF cells. *A*, immunoblot of caspase-1 in VZV (recombinant parent Oka)-infected HELF cells. Active caspase-1 subunit (p20) was detected in VZV-infected HELFs but not in the mock-infected cells. *B*, active caspase-1 visualization with 10 μ M biotinylated peptide caspase-1 inhibitor YVAD in the rOka-ORF10-GFP-infected HELF cells. Active caspase-1 was stained with biotinylated YVAD and detected with streptavidin conjugated to Texas Red. Active caspase-1 (red) was labeled in the VZV-infected HELF cells but not in the mock-infected cells. Hoechst staining was used to detect the nuclei (blue). The inset (orange square) indicates the red that is shown at higher magnification in the right panel. Uninfected cells (lower panel) were used as a negative control. *C*, ELISA measurement of secreted IL-1 β from HELF cells in the presence or absence of LPS. VZV-infected and uninfected HELFs were treated with the caspase-1 inhibitor Boc-D-CMK (50 μ M), the proteasomal inhibitor MG132 (10 μ M), or the potassium efflux inhibitor extracellular KCl (130 mM) in the presence of 1 μ g/ml LPS. ELISA data represent two independent experiments with samples measured in triplicate in each; the error bars represent the S.E. *D*, VZV infection alone induced pro-IL-1 β expression and processing in HELF cells. VZV-infected and uninfected HELFs were used to test for the effects of VZV infection (with and without LPS) on pro-IL-1 β expression and processing. VZV infection up-regulated and induced the processing of IL-1 β in the presence and in the absence of LPS (1 μ g/ml) as indicated by the detection of the pro-IL-1 β and the IL-1 β processed form (p17). 50 μ M caspase-1 inhibitor Boc-D-CMK was sufficient to block the caspase-1 enzymatic activity and to prevent the processing of IL-1 β in VZV-infected LPS-treated and LPS-untreated HELF cells as indicated by the detection of the processed form (p17) of IL-1 β .

defined by cytopathic changes, including formation of syncytia and the expression of the VZV ORF23 capsid protein detected by staining with anti-VZV-ORF23 polyclonal antibody. Tissue sections were imaged with a Leica TCS^{SP2} confocal microscope.

RESULTS

VZV Activates Caspase-1 and Induces Processing of IL-1 β in Human Fibroblasts—HELFs were inoculated with VZV-infected HELFs for 24 h, and expression of activated caspase-1 was assessed by immunoblot when ~75% of HELFs were

infected. Activation of caspase-1 was shown by the detection of caspase-1 p20, which is one of the active caspase-1 subunits, in VZV-infected cells but not in control HELFs (Fig. 1A). To further confirm that VZV activated caspase-1, HELFs were infected with VZV and stained with biotinylated YVAD, which is a peptide inhibitor of activated caspase-1 and binds specifically to this form of the protein. As shown in Fig. 1B, activated caspase-1 was readily detected in HELFs infected with VZV using rOka-ORF10-GFP to identify infected cells. Release of IL-1 β into culture supernatants demonstrates that caspase-1 is activated and functional (28, 29). IL-1 β was detected in supernatants recovered from VZV-infected cells but not from mock-infected HELFs in the presence or absence of LPS (Fig. 1C), which was consistent with the detection of activated caspase-1 shown in Fig. 1, A and B. IL-1 β secretion from VZV-infected HELFs was enhanced in the presence of LPS (1 μ g/ml). These findings of caspase-1 activation and IL-1 β secretion provided evidence of inflammasome induction in response to VZV infection of HELFs.

Several agents are known to interfere with inflammasome function. Most of these inhibitors block either active caspase-1, *e.g.* the peptide inhibitor YVAD and the chemical inhibitor Boc-D-CMK, or prevent potassium ion efflux, *e.g.* glibenclamide (30) and extracellular KCl (31). Proteasomal inhibitors, such as MG132, have also been reported to block activation of the inflammasome (32) presumably by preventing proteasomal degradation of unidentified inflammasome-regulatory protein(s). These agents were used to investigate whether IL-1 β processing and release by VZV-infected cells required caspase-1 activation as expected for an inflammasome-mediated under "Experimental Procedures." As shown in Fig. 1C, treatment with MG132 (10 μ M) reduced the IL-1 β concentration to levels found in supernatants from HELFs that were mock-infected and treated with MG132. Treatment with extracellular KCl (130 mM) and Boc-D-CMK (50 μ M) also prevented IL-1 β processing in VZV-infected HELFs, reducing secretion to background levels (Fig. 1C). The higher background for HELFs treated with different inflammasome-inhibiting conditions is likely to reflect some associated cell toxicity. These results suggested that VZV induces an inflammasome complex with activated caspase-1 in HELFs and requires potassium ion efflux and functional proteasomes to catalyze the processing of pro-IL-1 β .

LPS is a potent stimulant of innate responses, inducing pro-inflammatory cytokines and enhancing IL-1 β secretion (33–36). We compared the induction of IL- β and IL-1 β processing in VZV-infected HELFs with and without LPS treatment (1 μ g/ml) and in the presence and absence of 50 μ M Boc-D-CMK, an inhibitor of active caspase-1 (Fig. 1D). Pro-IL-1 β was present at low levels in uninfected, untreated HELFs and was not increased by exposure to the relatively low concentration of LPS used in these experiments. VZV-infected cells had higher levels of expression of pro-IL-1 β compared with uninfected HELFs, and expression was increased somewhat more when infected cells were also treated with LPS. IL-1 β processing also occurred in VZV-infected cells with and without LPS stimulation as shown by detection of the p17 subunit of IL-1 β (Fig. 1D). These results showed that VZV increased pro-IL-1 β synthesis and confirmed that VZV alone, without the need for another

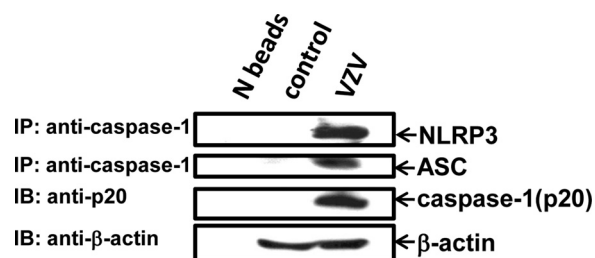


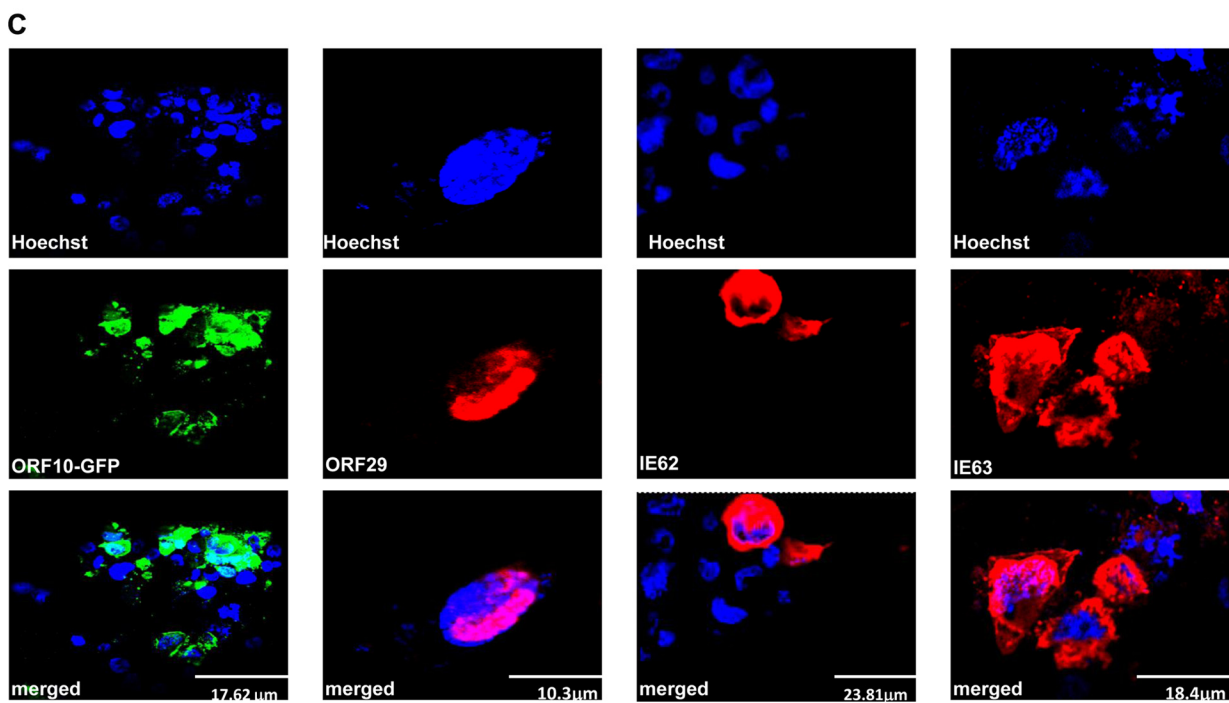
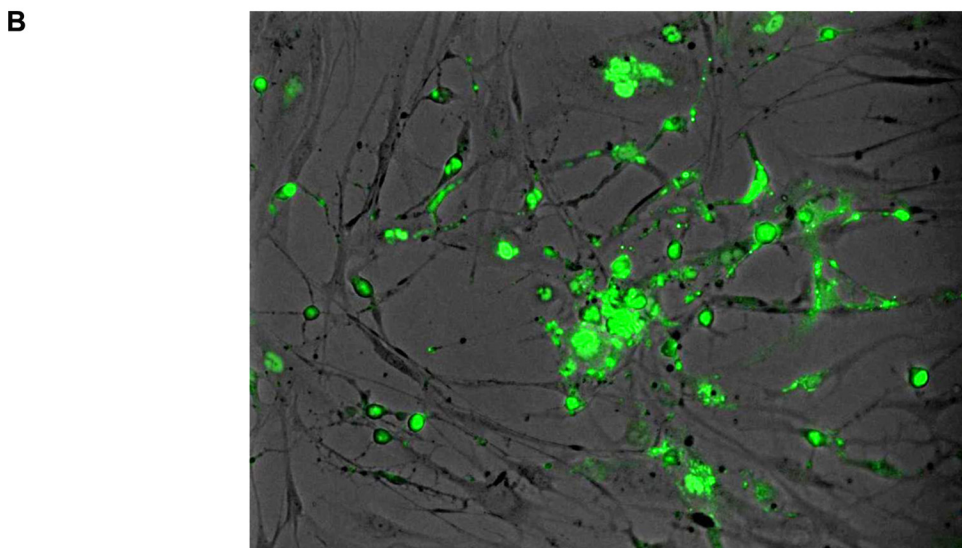
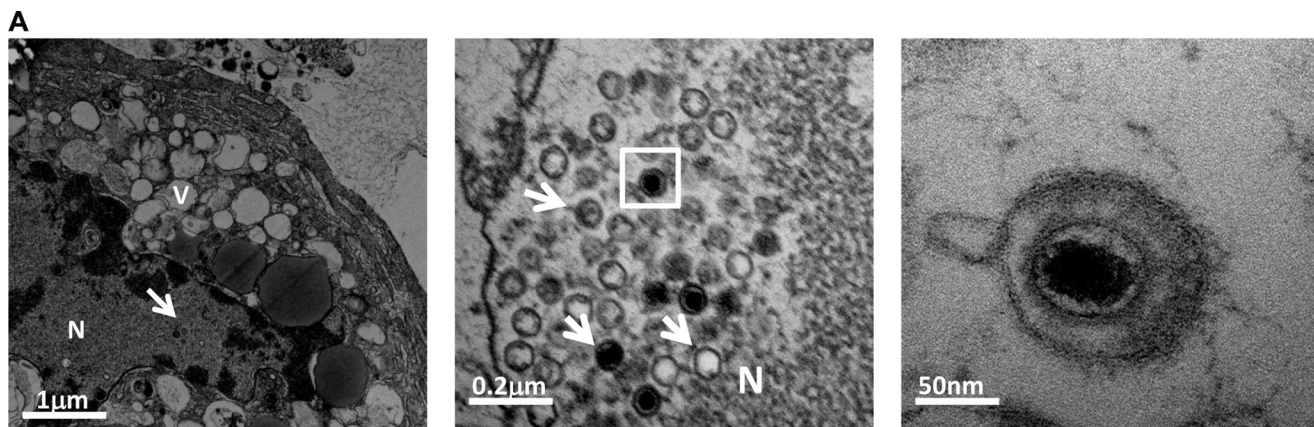
FIGURE 2. Immunoprecipitation of caspase-1 complex from VZV-infected HELF cells. HELF cells infected with VZV (recombinant parent Oka) activated caspase-1 as indicated by the presence of p20 in the infected lysate. Using cross-linked anti-caspase-1 antibody, both NLRP3 and the adaptor protein ASC were pulled down with the immunoprecipified caspase-1 complex from the VZV-infected HELF lysate. Uninfected HELF cells and normal rabbit IgG, pre-immune IgG cross-linked to agarose beads (*N beads*), were used as negative controls. *IP*, immunoprecipitation; *IB*, immunoblot.

trigger of inflammasome formation, was associated with processing of pro-IL1 β in HELFs.

VZV Induces Formation of NLRP3 Inflammasome in Human Fibroblasts—Because the NLRP3 inflammasome is reported to be involved in sensing of several viruses (7, 37, 38), we hypothesized that VZV induces this inflammasome complex in HELFs. To test this hypothesis, caspase-1 was immunopurified from VZV-infected and uninfected HELFs using a cross-linked anti-caspase-1 antibody column, and anti-NLRP3 and anti-ASC antibodies were used to probe the immunoblot for the other components of the complex. As shown in Fig. 2, both NLRP3 and ASC were detected in the lysate of VZV-infected HELFs eluted from the anti-caspase-1 column but not from uninfected HELF lysate or the column with cross-linked preimmune rabbit IgG. The presence of activated caspase-1 (p20 subunit) in the VZV-infected cell lysate was confirmed. This result demonstrated the formation of the active caspase-1 complex and suggested that NLRP3 is involved in sensing VZV in HELFs.

VZV Activates Caspase-1 in THP-1 Cells—THP-1 cells, a transformed human monocyte cell line, have been used extensively for studying human inflammasome formation (10). To determine whether VZV induction of the NLRP3 inflammasome could be investigated in these cells, we first assessed whether THP-1 cells were permissive for VZV replication. THP-1 cells were infected with rOka-ORF10-GFP, and GFP-positive and -negative cells were sorted by flow cytometry. The VZV-positive sorted cells were examined for virus production in THP-1 cells by EM. As shown in Fig. 3A, VZV capsids at various stages of maturation, including empty capsids, capsids with a translucent core, and capsids containing packaged DNA, and enveloped virions (Fig. 3A, right panel) were detected in THP-1 cell nuclei. To confirm that THP-1 cells could produce infectious virus progeny, HELFs were inoculated with the infected, sorted THP-1 cells (1:10 ratio). As shown in Fig. 3B, VZV plaques were formed in the HELF monolayer. Infected THP-1 cells were also analyzed for the expression of two immediate early VZV proteins, IE62 and IE63; the single-stranded DNA-binding protein ORF29, which is a marker for VZV replication compartments in the infected cell nucleus; and the late ORF10 protein (Fig. 3C); as expected for permissive cells, all of these viral proteins were expressed in VZV-infected THP-1 cells.

VZV Triggers Inflammasome Formation



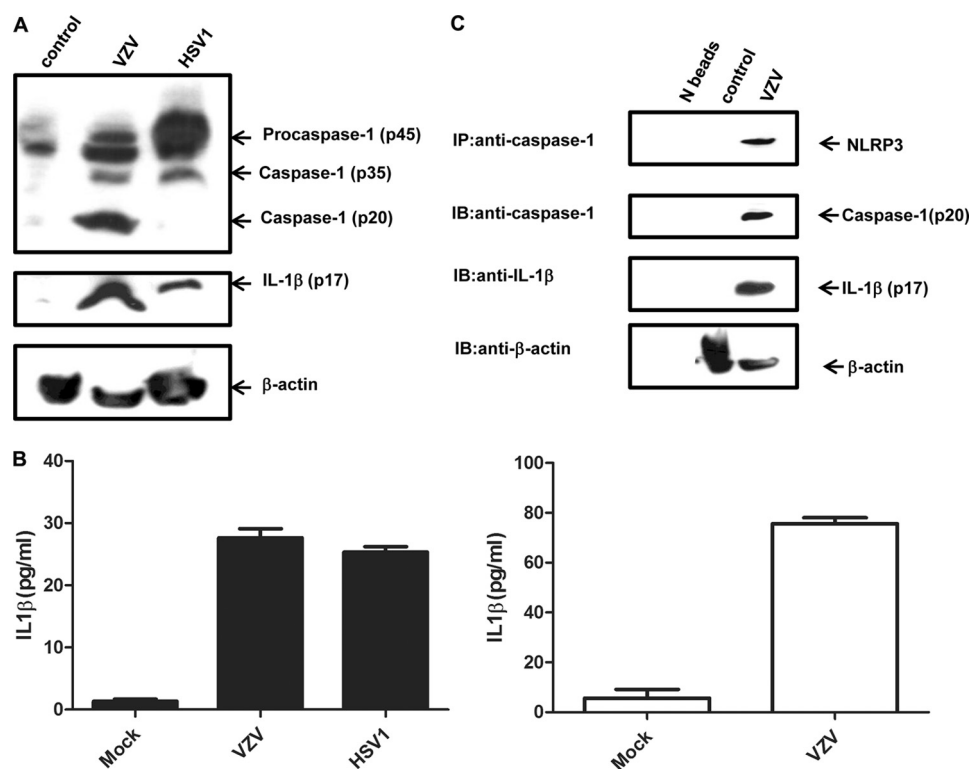


FIGURE 4. Activation of caspase-1 in VZV-infected THP-1 cells. *A*, detection of caspase-1 activity in VZV- and HSV-1-infected THP-1 cells. THP-1 cells were infected with the sorted VZV ORF10-GFP-positive cells for 24 h; for HSV-1 infection, THP-1 cells were infected with HSV-1 (multiplicity of infection of 10) for 12 h. Immunoblotting of THP-1 cells infected with VZV or HSV-1 using anti-caspase-1 antibody detected p35, an intermediate of active caspase-1 in the infected THP-1 cells but not in the mock, uninfected THP-1 cells. The processed form of IL-1 β (p17) was detected in the cell lysates of VZV- and HSV-1-infected THP-1 cells, indicating formation of an active caspase-1 complex in these infected cells. *B*, ELISA measurement of IL-1 β secretion in the supernatants of VZV- and HSV-1-infected THP-1 cells in the absence (*left panel*) of LPS and for the VZV in the presence (*right panel*) of 1 μ g/ml LPS. ELISA data represent two independent experiments with triplicate samples in each; the *error bars* represent S.E. *C*, immunoprecipitation of caspase-1 complex from THP-1 lysate. A cross-linked anti-caspase-1 antibody column was used to immunoprecipitate caspase-1 complex from VZV-infected and uninfected THP-1 lysates. NLRP3 protein was detected in the eluate only of the VZV-infected THP-1 lysate. The activity of caspase-1 in the lysate was judged by the presence of the p20 subunit of caspase-1 and the processed form of IL-1 β (p17). Uninfected THP-1 lysate and preimmune rabbit IgG, normal antibody cross-linked to agarose beads (*N beads*), were used as negative controls. *IP*, immunoprecipitation; *IB*, immunoblot.

To investigate caspase-1 activation, VZV-infected THP-1 cells were used to inoculate uninfected THP-1 cells for 24 h. Although PMA is commonly used to induce the differentiation of THP-1, PMA is an inducer of ROS release (39, 40), which could modify the cysteine residues of the active sites of many cellular enzymes, including caspase-1 (41, 42). Moreover, PMA is also known to up-regulate expression of AIM2 (21), a cytoplasmic receptor of double-stranded DNA that activates caspase-1. Therefore, PMA was avoided in these experiments. As shown in Fig. 4*A*, VZV activated caspase-1 in THP-1 cells as indicated by the presence of the active caspase-1 subunit, p20, and by the detection of the processed form of IL-1 β (p17) in infected cell lysates. HSV-1 also activated caspase-1 in THP-1 cells as indicated by the presence of the intermediate active caspase-1 subunit, p35, and induced the processing of IL-1 β in

infected THP-1 cells (Fig. 4*A*). These results were confirmed by detection of IL-1 β in infected cell supernatants from THP-1 cells infected with VZV and HSV (Fig. 4*B*, *left panel*). Because LPS and PMA were not used in these THP-1 cultures infected with VZV or HSV-1, the amount of secreted IL-1 β was low. When sorted THP-1 cells were used to infect uninfected THP-1 cells followed by 1 μ g/ml LPS treatment for 2 h before measuring the secreted IL-1 β in supernatants of the VZV-infected and uninfected THP-1 cells, more IL-1 β was detected (Fig. 4*B*, *right panel*), confirming the results in HELFs (Fig. 1*D*). This result confirmed that LPS is not required for the release of the processed IL-1 β , but it enhances its secretion. A possible explanation for why the amount of detected IL-1 β secreted from VZV-infected THP-1 cells is low compared with VZV-infected HELF cells

FIGURE 3. VZV replication and production of virus progeny in THP-1 cells. *A*, electron microscopy of VZV-infected THP-1 cells. THP-1 cells infected with the ORF10-GFP-expressing rOka virus were examined 24 h after infection. The *left panel* shows an overview of an infected THP-1 cell (low magnification; *scale bar*, 1 μ m). *N* indicates the nucleus, and *V* indicates vacuoles. The *middle panel* shows capsid maturation in an infected THP-1 nucleus. *Arrows* indicate different stages of VZV capsid maturation, including empty capsids, capsids with a translucent core, and capsids containing packaged DNA. The *right panel* shows an enveloped VZV virion at higher magnification (*scale bar*, 50 nm). The area in the *white square* of the *middle panel* (*scale bar*, 0.2 μ m) is shown at higher magnification in the *right panel*. *B*, rOka-ORF10-GFP-infected THP-1 cells transmitted rOka-ORF10-GFP virus to uninfected HELF cells. Infected THP-1 cells were used to inoculate uninfected HELF cells (one infected THP-1 cell to 10 uninfected HELF cells). GFP protein was expressed in HELF cells after 4 days of incubation, indicating VZV infection. Infected cells are *green*, and uninfected cells are *gray* (phase-contrast). *C*, detection of VZV protein expression in the infected THP-1 cells. Sorted THP-1 cells, infected with rOka-ORF10-GFP, were subjected to immunostaining for VZV immediate early proteins (IE62 and IE63) and ORF29, a single-stranded DNA-binding protein, as an early protein. The late protein, ORF10, was expressed as GFP fusion protein. Infected THP-1 cells expressed IE62 and IE63 (*red*), ORF29 (*red*), and ORF10 (*green*). Hoechst staining (*blue*) was used to detect the nuclei. Uninfected cells served as a staining control.

VZV Triggers Inflammasome Formation

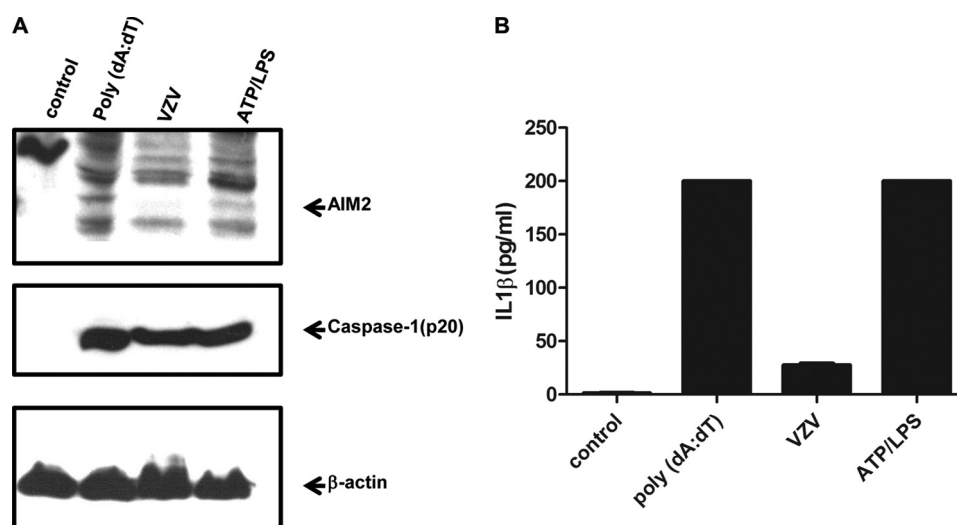


FIGURE 5. AIM2 protein expression in VZV-infected THP-1 cells. *A*, immunoblot detection of the AIM2 protein expression in VZV-infected THP-1 cells. Sorted THP-1 cells infected with VZV (rOka-ORF10-GFP) were probed for AIM2 protein expression. PMA-differentiated THP-1 cells treated with ATP/LPS and PMA-differentiated THP-1 cells transfected with poly(dA:dT), a ligand of AIM2, were used as positive controls. VZV infection did not induce AIM2 up-regulation in THP-1 cells, unlike the PMA-differentiated THP-1 cells transfected with poly(dA:dT) and those treated with ATP/LPS. Caspase-1 activity in the lysates was detected by the anti-caspase-1 (p20) antibody. *B*, ELISA measurement of the secreted IL-1 β in the supernatant of VZV-infected, poly(dA:dT)-transfected, and ATP/LPS-treated THP-1 cells. ELISA data represent two independent experiments with triplicate samples in each; the error bars represent S.E.

(Figs. 1C and 4B) is the binding of the secreted IL-1 β by the IL-1 receptors on uninfected THP-1 cells.

When the formation of the NLRP3 inflammasome in VZV-infected THP-1 cells was evaluated by immunoprecipitation using an anti-caspase-1 column, NLRP3 was shown to be present in the caspase-1 complex but was not detected in uninfected THP-1 cells (Fig. 4C). Activated caspase-1, detected as the p20 subunit, as well as processed IL-1 β , detected as the p17 form of the protein, was confirmed to be present in the initial infected THP-1 cell lysates by immunoblot (Fig. 4C).

VZV Triggers Formation of Activated Caspase-1 Inflammasome Complex in Absence of AIM2—The AIM2 protein recognizes double-stranded DNA (dsDNA) of several pathogens, including vaccinia virus, which, unlike VZV, replicates in the cytoplasm, and caspase-1 is activated by an AIM2-ASC complex (21, 43). In human monocytes, AIM2 expression requires induction by interferons (8). Because the activation of caspase-1 in VZV-infected cells might occur through AIM2-ASC complex formation, we investigated whether AIM2 was induced in VZV-infected THP-1 cells. As shown in Fig. 5A, VZV did not up-regulate AIM2 in THP-1 cells, although caspase-1 was active as indicated by the presence of the p20 subunit. The secretion of IL-1 β into supernatants of VZV-infected THP-1 cell cultures was confirmed (Fig. 5B); positive controls included poly(dA:dT)-transfected and ATP/LPS-treated THP-1 cells. Because AIM2 is induced by type I IFNs, we analyzed cytokine release from VZV-infected and uninfected THP-1 cells using a multiplex (Luminex) assay. Type I IFN secretion did not differ between mock-infected and VZV-infected THP-1 cells (data not shown). The human MxA is a sensitive marker for type I IFN induction (44). As shown in Fig. 6A, VZV-infected THP-1 cells did not show up-regulation of the IFN-induced form of MxA in contrast to the control THP-1 cells, which were transfected with poly(dA:dT), a known IFN inducer (45). This result is consistent with our observation that VZV blocks IRF3 expression in HELF cells (46).

AIM2 expression has been reported to be absent in melanoma cells (47). To confirm that the melanoma cells (MeWo) used in these experiments did not express AIM2, we transfected these cells with poly(dA:dT). We avoided using VZV genomic DNA in this experiment because VZV DNA alone is infectious. As shown in Fig. 6B, poly(dA:dT) induced the type I IFN pathway as indicated by up-regulation of MxA protein expression; however, this condition failed to induce caspase-1 activation compared with THP-1 cells transfected with poly(dT:dA). This result confirms that MeWo cells lack the AIM2-dependent sensor(s) of dsDNA that induces caspase-1 activation; however, the cells can respond to dsDNA to induce IFN signaling. Moreover, AIM2 expression was not detected in dsDNA-transfected MeWo cells (data not shown). When caspase-1 activation was evaluated in VZV-infected melanoma cells, activated caspase-1 was detected using the biotinylated caspase-1 peptide inhibitor YVAD in melanoma cells infected with VZV for 36 h (Fig. 7A, upper panels) but not in the uninfected cells (control; Fig. 7A, lower panel). When formation of the NLRP3 inflammasome was evaluated 24 h after VZV infection of melanoma cells, NLRP3 and ASC were detected in the immunoprecipitated complex (Fig. 7B). These results confirmed the observations from VZV-infected HELF and THP-1 cells, suggesting that the NLR protein NLRP3 is involved in sensing VZV pathogen-associated molecular patterns or danger-associated molecular patterns.

Because the NLRP3 inflammasome has been reported to be regulated by free radical ROS (48), we hypothesized that VZV might induce ROS release, which in turn would induce formation of the NLRP3 complex. To test this hypothesis, melanoma cells were infected with VZV for 24 h and stained with CM-H₂DCFDA, a fluorescent probe for ROS. No significant amount of ROS was detected (Fig. 7C). These experiments in melanoma cells suggest that VZV activates the NLRP3 inflammasome complex by a mechanism that is independent of AIM2 and oxidative stress.

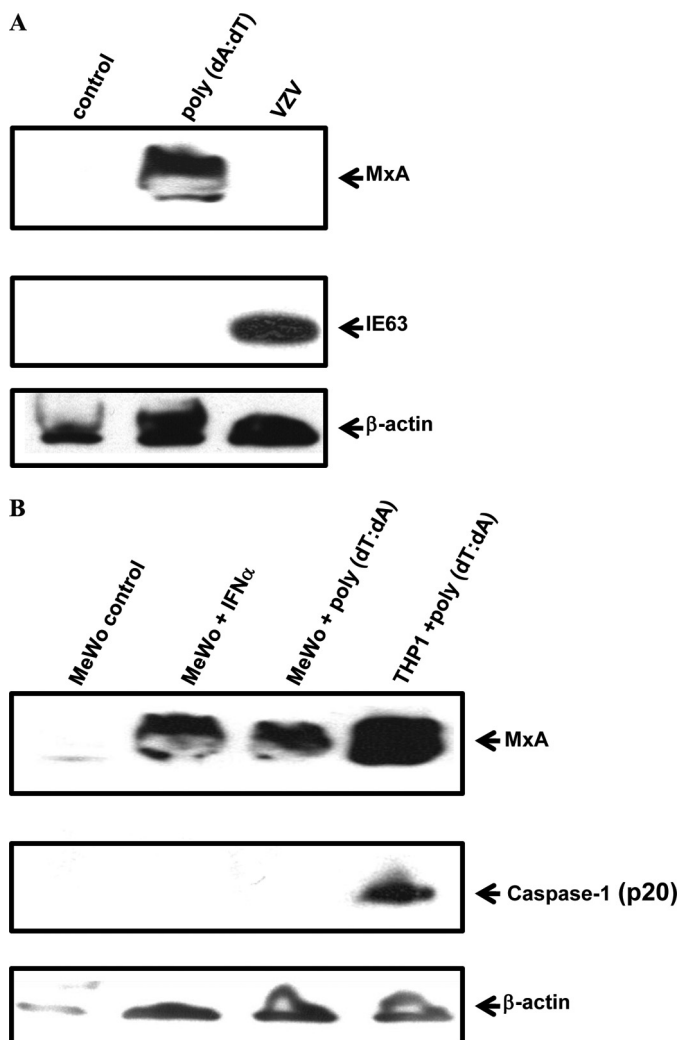


FIGURE 6. dsDNA transfection activates caspase-1 in THP-1 but not in melanoma cells. *A*, immunoblot detection of MxA protein expression in VZV-infected THP-1 cells. Sorted THP-1 cells infected with VZV (rOka-ORF10-GFP) were probed for MxA protein expression. PMA-differentiated THP-1 cells transfected with 1 μ g/ml poly(dA:dT), a ligand for AIM2 and a robust inducer of type I interferon, were used as a positive control. Mock-infected THP-1 cells were used as a negative control. No MxA protein expression was detected in VZV-infected THP-1 cells as a consequence of blocking the type I interferon response; however, THP-1 cells transfected with dsDNA activated caspase-1 and up-regulated MxA protein. *B*, immunoblot detection of caspase-1 activity in melanoma cells after transfection with double-stranded DNA. Melanoma cells were transfected with 1 μ g/ml poly(dT:dA). No caspase-1 activity was detected in melanoma cells transfected with dsDNA, although MxA protein was up-regulated in the cells, indicating that dsDNA transfection induced type I secretion and up-regulated MxA but not AIM2 protein. Melanoma cells treated with 1000 units/ml IFN- α were used as a positive control for MxA expression. THP-1 cells transfected with 1 μ g/ml poly(dT:dA) were used as a positive control for MxA up-regulation and caspase-1 activation. Untreated melanoma cells served as a negative control.

NLRP3 Expression in VZV-infected Skin Xenografts in Vivo—Expression of NLR proteins is tissue-restricted (49). NLRP3 has been reported to be weakly expressed in skin keratinocytes (49). Based on the results in cultured cells infected with VZV *in vitro*, we examined NLRP3 expression in human skin xenografts in SCID mice. Skin sections were tested for NLRP3 expression 7 days after VZV infection. By immunohistochemistry, NLRP3 was induced after VZV infection (Fig. 8A) but was not expressed in mock-infected normal skin xenografts. NLRP3

was detected in cells expressing VZV proteins (identified by staining with a polyclonal human anti-VZV antiserum) but not in the neighboring uninfected epidermal cells in the same sections. NLRP1 expression was not induced in VZV lesions (data not shown). NLRP3 up-regulation in lesions formed by VZV infection of skin xenografts was also detected by immunofluorescence using ORF23 expression as the marker of VZV infection (Fig. 8B). Interestingly, NLRP3 was detected in the nucleus as well as the cytoplasm of cells within the skin lesions. It is not clear whether NLRP3 protein is actively translocated into the nucleus under these conditions or reaches the nucleus because of VZV disruption of the nuclear membranes of infected skin cells. However, these results indicate that VZV infection induces NLRP3 expression in lesions in human skin xenografts *in vivo*.

DISCUSSION

Innate immune recognition of pathogens induces proinflammatory cytokines, type I IFNs, or both. In this study, we report that VZV activated the NLRP3 inflammasome in three cell types, including fibroblasts, THP-1, and melanoma cells that are permissive for VZV replication *in vitro*. In these cells, VZV DNA was not required for caspase-1 activation. Furthermore, activation of the NLRP3 inflammasome did not require ROS release in melanoma cells.

The NLRP3 inflammasome is activated by a broad range of microorganisms, including influenza virus (38), adenovirus (7), *Candida albicans* (50), *Staphylococcus aureus* (51), and *Listeria monocytogenes* (52). Microbial components, such as muramyl dipeptide and bacterial pore-forming toxins, can also activate the NLRP3 inflammasome (53, 54). In addition, host-derived stress signals, such as extracellular ATP (55), monosodium urate (56), and amyloid- β (57), as well as silica, asbestos, aluminum hydroxide, and many pollutants can elicit formation of the NLRP3 inflammasome (58, 59). Inflammasome formation leads to activation of procaspase-1 (p45), formation of heterotetramers of p10/p20 subunits of the procaspase-1, and the processing and release of the inflammatory cytokines that regulate the adaptive immune response (60, 61).

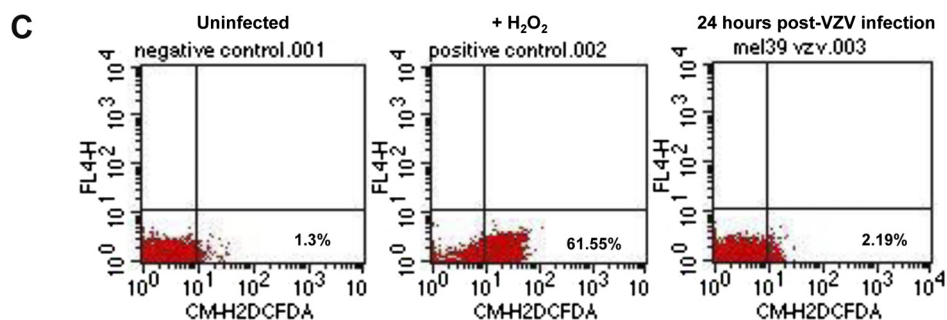
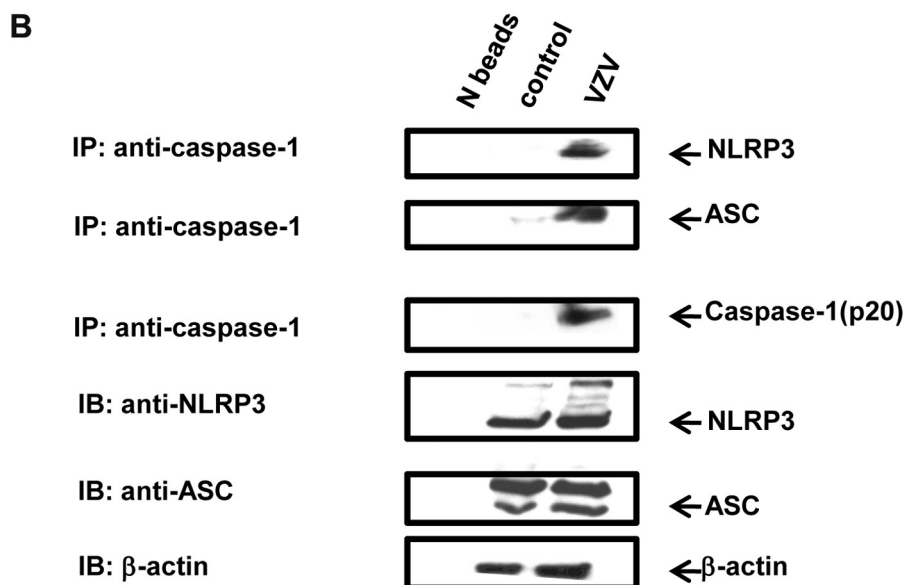
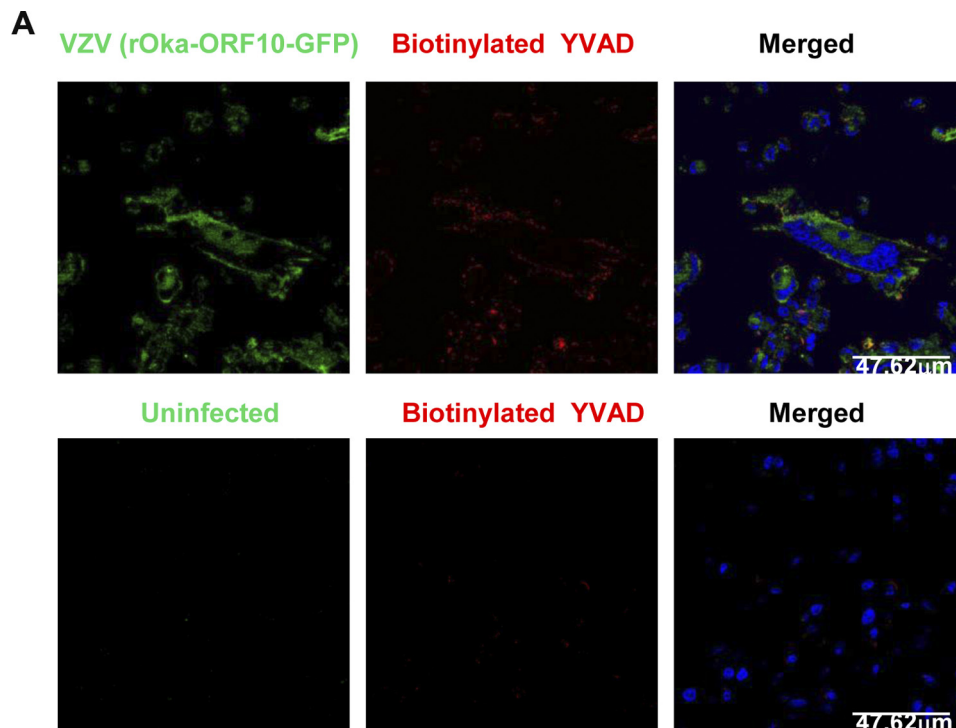
Like many viral pathogens, VZV infection is characterized by local inflammatory reactions, which are obvious at the sites of replication in skin, and proinflammatory cytokines are present in the peripheral blood of infected subjects (62–65). Our experiments help to account for these observations by establishing that VZV triggers assembly of an inflammasome complex. As defined in human fibroblasts, this process required potassium efflux and proteasome function. Moreover, VZV, like RNA viruses (37) and other DNA nuclear replicating viruses (7), was recognized by NLRP3 protein. Whether other NLR proteins also function in inflammasome complex formation in VZV-infected cells is not excluded and warrants further study.

The local inflammatory response recruits circulating monocytes, dendritic cells, and macrophages to sites of infection (66). Dendritic cells and macrophages isolated from human sources are known to be permissive for VZV replication (67). We used THP-1 cells to determine whether VZV infection of this cell type might be associated with inflammasome formation. THP-1 cells supported VZV replication, and VZV infection was

VZV Triggers Inflammasome Formation

associated with the formation of a functional NLRP3 inflammasome as determined by the occurrence of IL-1 β processing and secretion. HSV-1, another human alphaherpesvirus, also

induced activation of caspase-1 and secretion of IL-1 β by THP-1 cells. With regard to possible relevance for VZV pathogenesis, IL-1 β secretion up-regulates the surface expression of



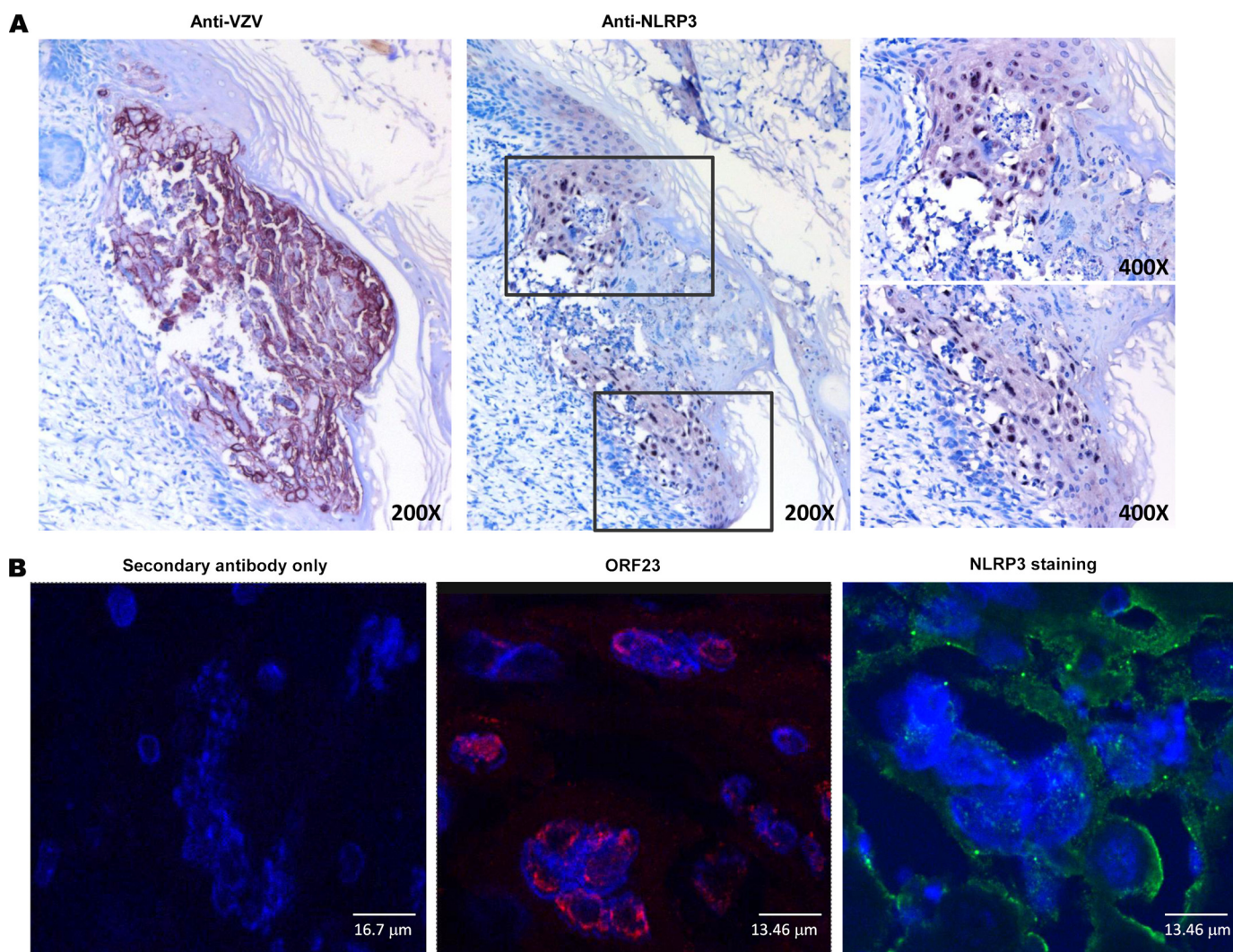


FIGURE 8. NLRP3 expression in human skin xenografts in human SCID mouse model of VZV pathogenesis. *A*, immunohistochemistry of NLRP3 expression in infected human skin xenografts in a human SCID mouse model. Formalin-fixed, paraffin-embedded sections (5 μm) of VZV-infected skin xenografts were stained with human polyclonal anti-VZV serum and detected with Vector VIP (purple) as shown in the left panel (magnification, $\times 200$). Methyl green, used as the counterstain, is visible in uninfected surrounding cells. NLRP3 antibody staining of a VZV lesion showed NLRP3 expression (purple) in the nuclei and the cytoplasm of VZV-infected skin xenografts. NLRP3 expression was not detected in uninfected areas (middle panel). The right panels are a higher magnification ($\times 400$) of the NLRP3-stained lesion in the middle panel. *B*, immunostaining of NLRP3 expression in infected human skin xenografts. The left panel shows the control staining with Alexa Fluor 488-conjugated anti-mouse secondary antibody alone. The middle panel shows the expression of the VZV protein ORF23 (red) in the lesion. The right panel shows the cytoplasmic and nuclear staining of the NLRP3 (green) in the infected lesion. Nuclei were stained with Hoechst (blue).

the adhesion molecules on both mesenchymal and endothelial cells. Surface expression of these adhesion molecules, along with secretion of chemokines, is required for recruitment of the circulating blood cells into infected tissues (60). We have shown that VZV infects T cells (27), allowing spread through the host, and causes skin lesions; VZV infection is presumed to be amplified by entry of uninfected T cells into skin sites of replication. Because IL-1 β also has adjuvant properties that enhance the adaptive

immune response, it is also likely to regulate the course of VZV infection so that it is rarely life-threatening to the host (10).

DNA viruses that replicate in the cytoplasm can activate caspase-1 through an alternative pathway involving formation of an AIM2/ASC inflammasome that lacks NLRP3 (8, 21). AIM2, which is not expressed in melanoma cells, is a cytoplasmic protein that belongs to the HIN-200 family, which is induced by type I IFNs (8, 68). Several herpesviruses, including VZV, block type I

FIGURE 7. Caspase-1 activity in VZV-infected melanoma cells. *A*, visualization of active caspase-1 in VZV-infected melanoma cells. Melanoma cells infected with rOka-ORF10-GFP for 36 h were stained with the biotinylated caspase-1 peptide inhibitor YVAD and detected with streptavidin conjugated to Texas Red. Active caspase-1 (red) was detected only in infected melanoma cells. VZV infection was indicated by the expression of the late protein, ORF10-GFP (green). Hoechst staining was used to detect the nuclei (blue). *B*, immunoprecipitation of caspase-1 complex using cross-linked anti-caspase-1 antibody. NLRP3 and ASC proteins were pulled down with the immunopurified caspase-1 complex from VZV-infected melanoma cells. The activity of caspase-1 in the lysate was judged by the detection of the active caspase-1 subunit (p20). Uninfected melanoma cells and preimmune rabbit IgG, normal antibody cross-linked to agarose beads (*N beads*), were used as negative controls. *C*, flow cytometry analysis of VZV-infected melanoma cells stained with the CM-H₂DCFDA, a detector of ROS release. VZV did not induce a significant amount of ROS release from VZV-infected melanoma cells compared with the uninfected cells and the positive control. Melanoma cells treated with 1% H₂O₂ were used as a positive control. The uninfected cells were used as a negative control. *IP*, immunoprecipitation; *IB*, immunoblot.

VZV Triggers Inflammasome Formation

IFNs (46, 69–71). Consistent with these studies, we found that VZV does not up-regulate AIM2 or MxA proteins in THP-1 cells, although it activated caspase-1. Moreover, caspase-1 was not activated in melanoma cells after transfection with dsDNA, whereas VZV infection activated the NLRP3 inflammasome, indicating that caspase-1 activation is independent of type I IFN induction and therefore of AIM2 in these cells. Consistent with our results, AIM2 is not the sensor of HSV-1 in macrophages (72). How NLRP3 senses diverse stimuli is not understood. Free radical ROS have been proposed to activate the NLRP3 inflammasome (48, 73, 74). Possible ROS sources include xanthine oxidase, peroxisomal oxidases, and NADPH oxidases that may be altered in virus-infected cells. However, ROS release was not detected in VZV-infected melanoma cells at a time point corresponding to the activation of caspase-1 in these cells. We concluded that ROS is not required for caspase-1 activation during VZV infection in melanoma cells. Interestingly, knocking out superoxide dismutase, an enzyme required for deactivation of ROS, results in high intracellular ROS and impairment of caspase-1 function (42). Moreover, patients with mutated NADPH oxidase, an enzyme required for the generation of ROS, show normal caspase-1 activation and IL-1 β secretion (75).

Taking advantage of our SCID mouse model of VZV pathogenesis, we found that NLRP3, unlike NLRP1, was induced in cells within VZV lesions in human skin xenografts, indicating that NLRP3 inflammasome formation occurs also in VZV-infected skin *in vivo*. However, whether inflammasome activation is beneficial for the host or required for effective spread of the virus is not known. Treatment of HSV-1-infected mice with IL-18, one of the substrates of active caspase-1, has been reported to protect against HSV-1 infection (76). Although it seems likely to be beneficial for enhancing the host adaptive immune response, caspase-1 activation also has been shown to be required for successful infection by bacterial pathogens (77).

In summary, we report that VZV is sensed by the innate cellular NLR mechanism, causing caspase-1 activation *in vitro* and in infected skin *in vivo*. This mechanism is functional even though the viral DNA-sensing proteins that are regulated by type I IFNs are blocked by VZV interference with the type I IFN response within infected cells. In contrast, we found that VZV triggers NLRP3 inflammasome formation and IL-1 β processing in different human cell lines that support VZV replication. NLRP3 inflammasome formation can be considered an immunomodulatory mechanism triggered by the virus that helps to support VZV persistence in the population by modifying the severity of infection in the individual. This proinflammatory mechanism is likely to be involved in the pathogenesis of infections caused by the other medically important human herpesviruses and might be targeted for enhancement by antiviral therapies.

Acknowledgments—We thank Dr. Jurgen Brojtsch, Albert Einstein College of Medicine, for suggestions. We also thank Kathy Crumpton and Tim Knaak from the FACS facility at Stanford University for technical assistance in sorting of THP-1 cells. We also thank Yael Rosenberg-Hasson, Human Immune Monitoring Center facility at Stanford University, for technical assistance to run the multiplex (Luminex) assay.

REFERENCES

1. Cohen, J. I., Straus, S. E., and Arvin, A. M. (2007) *Varicella-Zoster Virus*, 5th Ed., pp. 2773–2818, Lippincott Williams and Wilkins, Philadelphia
2. Mueller, N. H., Gilden, D. H., Cohrs, R. J., Mahalingam, R., and Nagel, M. A. (2008) *Neurol. Clin.* **26**, 675–697, viii
3. Arvin, A. M., Koropchak, C. M., Williams, B. R., Grumet, F. C., and Fong, S. K. (1986) *J. Infect. Dis.* **154**, 422–429
4. Torigo, S., Ihara, T., and Kamiya, H. (2000) *Microbiol. Immunol.* **44**, 1027–1031
5. Lund, J., Sato, A., Akira, S., Medzhitov, R., and Iwasaki, A. (2003) *J. Exp. Med.* **198**, 513–520
6. Lagos, D., Vart, R. J., Gratrix, F., Westrop, S. J., Emuss, V., Wong, P. P., Robey, R., Imami, N., Bower, M., Gotch, F., and Boshoff, C. (2008) *Cell Host Microbe* **4**, 470–483
7. Muruve, D. A., Pétrilli, V., Zaiss, A. K., White, L. R., Clark, S. A., Ross, P. J., Parks, R. J., and Tschopp, J. (2008) *Nature* **452**, 103–107
8. Hornung, V., Ablasser, A., Charrel-Dennis, M., Bauernfeind, F., Horvath, G., Caffrey, D. R., Latz, E., and Fitzgerald, K. A. (2009) *Nature* **458**, 514–518
9. Gay, N. J., and Gangloff, M. (2007) *Annu. Rev. Biochem.* **76**, 141–165
10. Martinon, F., Mayor, A., and Tschopp, J. (2009) *Annu. Rev. Immunol.* **27**, 229–265
11. Martinon, F. (2007) *Eur. J. Immunol.* **37**, 3003–3006
12. Bryant, C., and Fitzgerald, K. A. (2009) *Trends Cell Biol.* **19**, 455–464
13. Di Virgilio, F. (2007) *Trends Pharmacol. Sci.* **28**, 465–472
14. Arlehamn, C. S., Pétrilli, V., Gross, O., Tschopp, J., and Evans, T. J. (2010) *J. Biol. Chem.* **285**, 10508–10518
15. Pétrilli, V., Papin, S., Dostert, C., Mayor, A., Martinon, F., and Tschopp, J. (2007) *Cell Death Differ.* **14**, 1583–1589
16. Ghayur, T., Banerjee, S., Hugunin, M., Butler, D., Herzog, L., Carter, A., Quintal, L., Sekut, L., Talanian, R., Paskind, M., Wong, W., Kamen, R., Tracey, D., and Allen, H. (1997) *Nature* **386**, 619–623
17. Gurcel, L., Abrami, L., Girardin, S., Tschopp, J., and van der Goot, F. G. (2006) *Cell* **126**, 1135–1145
18. Shao, W., Yeretssian, G., Doiron, K., Hussain, S. N., and Saleh, M. (2007) *J. Biol. Chem.* **282**, 36321–36329
19. Fernandes-Alnemri, T., Yu, J. W., Datta, P., Wu, J., and Alnemri, E. S. (2009) *Nature* **458**, 509–513
20. Agostini, L., Martinon, F., Burns, K., McDermott, M. F., Hawkins, P. N., and Tschopp, J. (2004) *Immunity* **20**, 319–325
21. Bürckstümmer, T., Baumann, C., Blüml, S., Dixit, E., Dürnberger, G., Jahn, H., Planyavsky, M., Bilban, M., Colinge, J., Bennett, K. L., and Superti-Furga, G. (2009) *Nat. Immunol.* **10**, 266–272
22. Takahashi, M., Otsuka, T., Okuno, Y., Asano, Y., and Yazaki, T. (1974) *Lancet* **2**, 1288–1290
23. Cohen, J. I., and Seidel, K. E. (1993) *Proc. Natl. Acad. Sci. U.S.A.* **90**, 7376–7380
24. Ku, C. C., Che, X. B., Reichelt, M., Rajamani, J., Schaap-Nutt, A., Huang, K. J., Sommer, M. H., Chen, Y. S., Chen, Y. Y., and Arvin, A. M. (2011) *Immunol. Cell Biol.* **89**, 173–182
25. Nour, A. M., Yeung, Y. G., Santambrogio, L., Boyden, E. D., Stanley, E. R., and Brojtsch, J. (2009) *Infect. Immun.* **77**, 1262–1271
26. Reichelt, M., Brady, J., and Arvin, A. M. (2009) *J. Virol.* **83**, 3904–3918
27. Ku, C. C., Zerboni, L., Ito, H., Graham, B. S., Wallace, M., and Arvin, A. M. (2004) *J. Exp. Med.* **200**, 917–925
28. Thornberry, N. A., Bull, H. G., Calaycay, J. R., Chapman, K. T., Howard, A. D., Kostura, M. J., Miller, D. K., Molineaux, S. M., Weidner, J. R., Aunins, J., Elliston, K. O., Ayala, J. M., Casano, F. J., Chin, J., Ding, G. J., Egger, L. A., Gaffney, E. P., Limjuco, G., Palyha, O. C., Raju, S. M., Rolando, A. M., Salley, J. P., Yamin, T. T., Lee, T. D., Shively, J. E., MacCross, M., Mumford, R. A., Schmidt, J. A., and Tocci, M. J. (1992) *Nature* **356**, 768–774
29. Perregaux, D., and Gabel, C. A. (1994) *J. Biol. Chem.* **269**, 15195–15203
30. Lamkanfi, M., Mueller, J. L., Vitari, A. C., Misaghi, S., Fedorova, A., Deshayes, K., Lee, W. P., Hoffman, H. M., and Dixit, V. M. (2009) *J. Cell Biol.* **187**, 61–70
31. Walev, I., Reske, K., Palmer, M., Valeva, A., and Bhakdi, S. (1995) *EMBO J.*

- 14, 1607–1614
32. Squires, R. C., Muehlbauer, S. M., and Brojtsch, J. (2007) *J. Biol. Chem.* **282**, 34260–34267
 33. Beuscher, H. U., Günther, C., and Rölinghoff, M. (1990) *J. Immunol.* **144**, 2179–2183
 34. Beutler, B. (2000) *Curr. Opin. Immunol.* **12**, 20–26
 35. Kakizaki, Y., Kraft, N., and Atkins, R. C. (1993) *Clin. Exp. Immunol.* **91**, 521–525
 36. Lovett, D. H., Bursten, S. L., Gemsa, D., Bessler, W., Resch, K., and Ryan, J. L. (1988) *Am. J. Pathol.* **133**, 472–484
 37. Ichinohe, T., Lee, H. K., Ogura, Y., Flavell, R., and Iwasaki, A. (2009) *J. Exp. Med.* **206**, 79–87
 38. Allen, I. C., Scull, M. A., Moore, C. B., Holl, E. K., McElvania-TeKippe, E., Taxman, D. J., Guthrie, E. H., Pickles, R. J., and Ting, J. P. (2009) *Immunity* **30**, 556–565
 39. Whitacre, C. M., and Cathcart, M. K. (1992) *Cell. Immunol.* **144**, 287–295
 40. Roy, S., Noda, Y., Eckert, V., Traber, M. G., Mori, A., Liburdy, R., and Packer, L. (1995) *FEBS Lett.* **376**, 164–166
 41. Kamata, H., Honda, S., Maeda, S., Chang, L., Hirata, H., and Karin, M. (2005) *Cell* **120**, 649–661
 42. Meissner, F., Molawi, K., and Zychlinsky, A. (2008) *Nat. Immunol.* **9**, 866–872
 43. Fernandes-Alnemri, T., Yu, J. W., Juliana, C., Solorzano, L., Kang, S., Wu, J., Datta, P., McCormick, M., Huang, L., McDermott, E., Eisenlohr, L., Landel, C. P., and Alnemri, E. S. (2010) *Nat. Immunol.* **11**, 385–393
 44. Haller, O., and Kochs, G. (2011) *J. Interferon Cytokine Res.* **31**, 79–87
 45. Hornung, V., and Latz, E. (2010) *Nat. Rev. Immunol.* **10**, 123–130
 46. Sen, N., Sommer, M., Che, X., White, K., Ruyechan, W. T., and Arvin, A. M. (2010) *J. Virol.* **84**, 9240–9253
 47. DeYoung, K. L., Ray, M. E., Su, Y. A., Anzick, S. L., Johnstone, R. W., Trapani, J. A., Meltzer, P. S., and Trent, J. M. (1997) *Oncogene* **15**, 453–457
 48. Zhou, R., Tardivel, A., Thorens, B., Choi, I., and Tschopp, J. (2010) *Nat. Immunol.* **11**, 136–140
 49. Kummer, J. A., Broekhuizen, R., Everett, H., Agostini, L., Kuijk, L., Martinon, F., van Bruggen, R., and Tschopp, J. (2007) *J. Histochem. Cytochem.* **55**, 443–452
 50. Joly, S., Ma, N., Sadler, J. J., Soll, D. R., Cassel, S. L., and Sutterwala, F. S. (2009) *J. Immunol.* **183**, 3578–3581
 51. Craven, R. R., Gao, X., Allen, I. C., Gris, D., Bubeck-Wardenburg, J., McElvania-TeKippe, E., Ting, J. P., and Duncan, J. A. (2009) *PLoS One* **4**, e7446
 52. Kim, S., Bauernfeind, F., Ablasser, A., Hartmann, G., Fitzgerald, K. A., Latz, E., and Hornung, V. (2010) *Eur. J. Immunol.* **40**, 1545–1551
 53. Martinon, F., Agostini, L., Meylan, E., and Tschopp, J. (2004) *Curr. Biol.* **14**, 1929–1934
 54. Silveira, T. N., and Zamboni, D. S. (2010) *Infect. Immun.* **78**, 1403–1413
 55. Franchi, L., Eigenbrod, T., and Núñez, G. (2009) *J. Immunol.* **183**, 792–796
 56. Martinon, F., Pétrilli, V., Mayor, A., Tardivel, A., and Tschopp, J. (2006) *Nature* **440**, 237–241
 57. Halle, A., Hornung, V., Petzold, G. C., Stewart, C. R., Monks, B. G., Reinheckel, T., Fitzgerald, K. A., Latz, E., Moore, K. J., and Golenbock, D. T. (2008) *Nat. Immunol.* **9**, 857–865
 58. Kool, M., Pétrilli, V., De Smedt, T., Rolaz, A., Hammad, H., van Nimwegen, M., Bergen, I. M., Castillo, R., Lambrecht, B. N., and Tschopp, J. (2008) *J. Immunol.* **181**, 3755–3759
 59. Hornung, V., Bauernfeind, F., Halle, A., Samstad, E. O., Kono, H., Rock, K. L., Fitzgerald, K. A., and Latz, E. (2008) *Nat. Immunol.* **9**, 847–856
 60. Dinarello, C. A. (2009) *Annu. Rev. Immunol.* **27**, 519–550
 61. Sims, J. E., and Smith, D. E. (2010) *Nat. Rev. Immunol.* **10**, 89–102
 62. Bannister, B., Gillespie, S. H., and Jones, J. (eds) (2006) *Infection Microbiology and Management*, 3rd Ed., Blackwell Publishing Ltd., Boston
 63. Bruder, E., Ersch, J., Hebisch, G., Ehrbar, T., Klimkait, T., and Stallmach, T. (2000) *Virchows Arch.* **437**, 440–444
 64. Shaikh, S., and Ta, C. N. (2002) *Am. Fam. Physician* **66**, 1723–1730
 65. Zhu, S. M., Liu, Y. M., An, E. D., and Chen, Q. L. (2009) *J. Zhejiang Univ. Sci. B* **10**, 625–630
 66. Springer, T. A. (1994) *Cell* **76**, 301–314
 67. Arbeit, R. D., Zaia, J. A., Valerio, M. A., and Levin, M. J. (1982) *Intervirology* **18**, 56–65
 68. Choubey, D., Walter, S., Geng, Y., and Xin, H. (2000) *FEBS Lett.* **474**, 38–42
 69. Hwang, S., Kim, K. S., Flano, E., Wu, T. T., Tong, L. M., Park, A. N., Song, M. J., Sanchez, D. J., O'Connell, R. M., Cheng, G., and Sun, R. (2009) *Cell Host Microbe* **5**, 166–178
 70. Jaworska, J., Gravel, A., Fink, K., Grandvaux, N., and Flamand, L. (2007) *J. Virol.* **81**, 5737–5748
 71. Joo, C. H., Shin, Y. C., Gack, M., Wu, L., Levy, D., and Jung, J. U. (2007) *J. Virol.* **81**, 8282–8292
 72. Rathinam, V. A., Jiang, Z., Waggoner, S. N., Sharma, S., Cole, L. E., Waggoner, L., Vanaja, S. K., Monks, B. G., Ganesan, S., Latz, E., Hornung, V., Vogel, S. N., Szomolanyi-Tsuda, E., and Fitzgerald, K. A. (2010) *Nat. Immunol.* **11**, 395–402
 73. Cassel, S. L., Eisenbarth, S. C., Iyer, S. S., Sadler, J. J., Colegio, O. R., Tephly, L. A., Carter, A. B., Rothman, P. B., Flavell, R. A., and Sutterwala, F. S. (2008) *Proc. Natl. Acad. Sci. U.S.A.* **105**, 9035–9040
 74. Dostert, C., Pétrilli, V., Van Bruggen, R., Steele, C., Mossman, B. T., and Tschopp, J. (2008) *Science* **320**, 674–677
 75. Meissner, F., Seger, R. A., Moshous, D., Fischer, A., Reichenbach, J., and Zychlinsky, A. (2010) *Blood* **116**, 1570–1573
 76. Fujioka, N., Akazawa, R., Ohashi, K., Fujii, M., Ikeda, M., and Kurimoto, M. (1999) *J. Virol.* **73**, 2401–2409
 77. Monack, D. M., Hersh, D., Ghori, N., Bouley, D., Zychlinsky, A., and Falkow, S. (2000) *J. Exp. Med.* **192**, 249–258